Evidence for 10^{18}-eV Neutral Particles from the Direction of Cygnus X-3

G. L. Cassiday, R. Cooper, B. R. Dawson, J. W. Elbert, B. E. Fick, K. D. Green, S. Ko, D. F. Liebing,
E. C. Loh, M. H. Salamon, J. D. Smith, P. Sokolsky, P. Sommers, and S. B. Thomas

Department of Physics, University of Utah, Salt Lake City, Utah 84112

(Received 15 September 1988)

Analysis of the cumulative Fly's Eye data reveals an excess of air showers from the direction of Cygnus X-3 at energies above 0.5×10^{18} eV. No point source has previously been identified at such high energies. The probability of this excess arising as a chance clustering of isotropic cosmic rays is 6.5×10^{-4}. The inferred signal flux is $(2.0 \pm 0.6) \times 10^{-17}$ particles/cm^2 s. The Cygnus X-3 4.8-h periodicity is weakly present in the data.

We report results from an analysis which examines the arrival directions of extensive air showers obtained by the Fly's Eye detectors.[1] Such a study could detect point sources of EeV (10^{18} eV) cosmic rays, since accelerated hadrons would produce neutral hadrons and γ rays through interactions with surrounding matter and infrared radiation. Cygnus X-3 is *a priori* the outstanding target of a point-source search since it is the one northern-hemisphere source which has been detected at energies as high as 10^{16} eV.[2,3] Numerous detections of Cygnus X-3 with air-shower techniques have been reported at energies ranging from 3×10^{11} eV up to 2×10^{16} eV.[4,5] Taken together, these detections indicate that the flux from Cygnus X-3 has a spectrum which is flatter than the cosmic-ray spectrum. The 4.8-h x-ray period has been featured in most of the detections, although there are also reports of unmodulated emissions from Cygnus X-3.[6,7] Intermittency of the detections suggests that the flux is episodic.

The Fly's Eye detectors located at latitude 40.2° in Dugway, Utah, have a 2π steradian angular acceptance and operate year round during moonless nights. The effective collecting area for the detection of showers by atmospheric scintillation grows with shower energy, starting at 0.1 EeV. Above 0.5 EeV, shower acceptance is not sensitive to small gain changes in the detector system. Only showers above this safe cut are included in the present analysis. The air-shower data set has been accumulated from November 1981, through May 1988, excluding the months from June through October of 1985, during which time the detectors were turned off for the installation of uv-passing filters. The data include 5609 well-reconstructed showers above 0.5 EeV. The second Fly's Eye has been operational since November 1986, and 1107 of the showers detected by both Eyes have been reconstructed with greater precision stereoscopically.

Evidence for an excess from the Cygnus X-3 direction emerges with little processing of the Fly's Eye data. In Fig. 1, shower counts are plotted as a function of galactic longitude for bins centered on the Cygnus X-3 galactic latitude. The Fly's Eye exposure accounts for the smooth variation of bin counts with longitude, but not the narrow excess near 80° where Cygnus X-3 lies.

For a detailed analysis of the shower excess at Cygnus X-3, we use a computational procedure which is intended to optimize sensitivity to point sources. It maximizes the usable data sample by taking advantage of shower-by-shower information about directional uncertainties. It deals with continuous functions on the sky and so avoids the difficulties inherent in procedures which segregate showers into discrete bins. A technique has also been developed for the handling of the Fly's Eye's irregular exposure in sidereal time. The analysis method will be explained in full elsewhere,[8] but a brief description follows. The hypothesis of cosmic-ray isotropy will be used in the evaluation of the expected intensity from the Cygnus X-3 region.

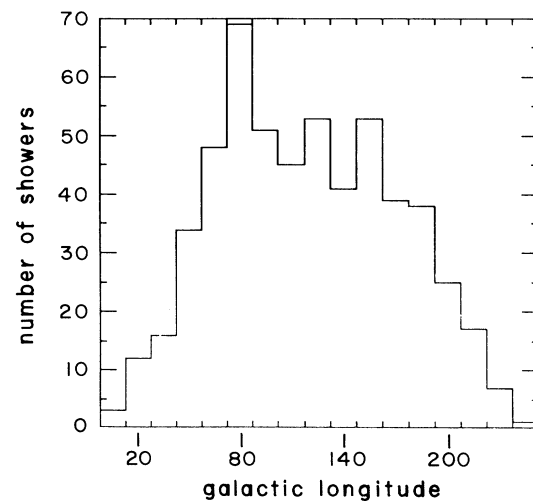Each shower's direction is represented by a probability

FIG. 1. The number of showers vs galactic longitude. Each bin is 10° wide in galactic latitude, with its center at latitude +1°. The bin with the most counts is centered to the nearest degree on Cygnus X-3.

distribution (or density function) on the celestial sphere. The distribution is centered on the shower's direction of origin given by the best-fit geometrical reconstruction, and the widths of the distribution depend on the errors associated with the determination of that direction. (For a typical shower, the constant-probability contours are highly elliptical because the shower's track across the sky determines a great circle with an average error of only $2°$, whereas an average error of $9°$ occurs in the determination of the direction of origin within the great circle.) At any point of the sky, summing of the density function for all showers gives the total shower density (showers/deg^2). Each shower's energy is represented by a probability distribution over energies, the width of which depends on the quality of the measured profile of its longitudinal development.[1] An energy cut can be implemented by multiplication of each shower's density function by the probability that its energy passes the cut. If the *weight* of a shower at a point of the sky is defined to be this rescaled density function evaluated at the point, then the total shower density at a point is simply the sum of all shower weights at that point. The smearing of each shower's energy reduces the dependence of results on the precise value of an energy cut, and the smearing of each shower's direction yields a continuous function for the total shower density, so no binning is required for its evaluation at any point of the sky. When the actual Fly's Eye data set is used to evaluate the total shower density at a point, that density will be called the *actual density* at the point.

Celestial anisotropies can be discerned by comparison of the actual data set with an ensemble of *simulation data sets* which are derived from the actual data set under the assumption that the Fly's Eye is responding to an isotropic particle intensity. If the particle intensity were isotropic, then there should be a time-independent flux from each direction in local detector coordinates (e.g., declination and hour angle). In that case, a shower detected with particular local coordinates could have arrived with equal probability at any other time of a shower detection. The simulation data sets simply exploit this property. Each simulation data set is constructed from the actual data set by our changing every shower's sidereal time of detection to a different value selected at random from the actual sidereal detection times, while preserving the shower's original declination and hour angle. For any point of the celestial sphere, the total shower density can be evaluated by each simulation data set, so the ensemble of simulation data sets determines a distribution of values for the density at that point. The mean value of that distribution defines the *expected density* at the point. The fraction of the simulation data sets in which the density exceeds the actual density measures the probability that a density as great as (or greater than) the actual density would occur if the particle intensity were isotropic.

These methods give a density excess at Cygnus X-3 of $68\% \pm 16\%$, with a chance probability of 6.5×10^{-4}. As one consistency check on the method, a similar probability evaluation was performed for an array of 1055 sky locations with a nearest-neighbor separation of $5°$. The distribution of these probabilities differs little[8] from a uniform distribution, and none of them was as low as the probability at Cygnus X-3.

The present study excludes showers with energies less than 0.5 EeV. Although the Fly's Eye detects showers of lower energy, the detector's acceptance increases rapidly with energy for such showers, and that energy dependence of the acceptance below 0.5 EeV has varied markedly with operating conditions. Special techniques will be necessary to study possible excesses below 0.5 EeV. Higher-energy cuts can be tried at the expense of reducing the data set. The statistical significance of the excess persists as the energy cut is moved from 0.5 to 4.0 EeV. For example, above 1 EeV the excess is $81\% \pm 24\%$ with a chance probability of 3.9×10^{-3}; above 2 EeV it is $170\% \pm 40\%$ with a probability of 9.0×10^{-4}; above 4 EeV it is $320\% \pm 71\%$ with a probability of 6.7×10^{-4}.

To determine the implied flux from Cygnus X-3, artificial signal showers were included in simulation data sets by our taking some randomly selected showers and moving them to the Cygnus X-3 location, but offset from it by sampling from each shower's angular error distribution. The number of artificial signal showers was adjusted until the mean density in those simulations matched the actual density at Cygnus X-3. This occurred when
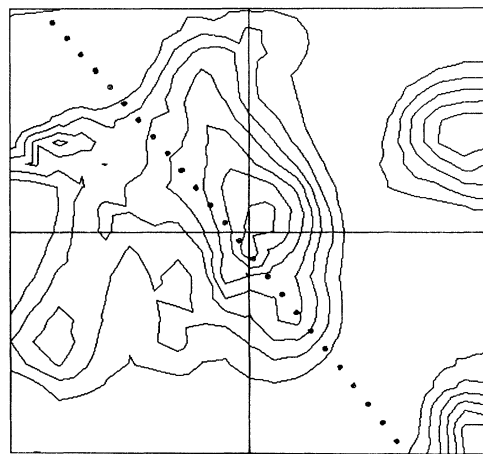

FIG. 2. Cygnus X-3 is at the center of this contour plot. The plot is $20° \times 20°$, with declination increasing vertically and right ascension increasing to the left. (The horizontal dimension is $20°$ true, not $20°$ of right ascension.) The dots are points of the galactic plane separated by $1°$ of longitude. The contour lines map the significance of shower density excess as described in the text. Their σ values are 1.0, 1.5, 2.0, 2.5, 3.0, 3.5, and 4.0.

the number of artificial signal showers above 0.5 EeV was 25 (which, because each shower has only a probability for being above 0.5 EeV, required an average of 60 artificial signal showers). The expected density at Cygnus X-3, based on the isotropic simulations without any artificial signal, is 0.26 showers/deg^2. Together with the known isotropic cosmic-ray intensity[9] of 6.8×10^{-6}/cm^2 s sr above 0.5 EeV, this gives an effective product of collecting area and running time equal to 1.25×10^{18} cm^2 s. The Cygnus X-3 flux above 0.5 EeV is then estimated to be

$$(25 \text{ showers})/(1.25 \times 10^{18} \text{ cm}^2 \text{ s}) = 2.0 \times 10^{-17}/\text{cm}^2 \text{ s}.$$

The uncertainty in this number is 30%. This arises in

part because of the 16% uncertainty in the 68% excess, which is evaluated by fluctuations in the isotropic simulations. Even if the 68% excess had no uncertainty, however, there is a spread in the number of showers (25 ± 6) which can produce the excess. (Relatively few artificial signal showers of high weight at Cygnus X-3 can produce the same excess as more such showers with lower weights.) Multiplication of the above particle flux by the minimum energy (0.5 EeV) gives an estimated energy flux of 10 eV/cm^2 s. If the source is 11 kpc away and emitting isotropically, this implies a power output of 2.3×10^{35} ergs/s.

Figure 2 shows the significance of the density excess as a function on the sky in a region centered on Cygnus X-3. The number of σ at any sky location is given by $(\rho_{act} - \rho_{sim})/\delta$. Here ρ_{act} is the actual density, ρ_{sim} is the expected density, and the denominator δ is the rms deviation of density values for that sky location. The function plotted in Fig. 2 should be compared with similar functions derived with simulations which include artificial signal showers, as described above. A quantitative way to do the comparison is to find the center and width of the Gaussian which best fits each function. In simulations, the centers are displaced from the true source location by an average 3.1°, whereas the offset is 2.6° for the function of Fig. 2. The excess plotted in Fig. 2 is found to be broader than the average simulation function, only 15% of the simulation functions having widths as great or greater.

The recent Molnar ephemeris[10] has been used for analysis of the Cygnus X-3 4.8-h periodicity. Figure 3 shows the phase dependence of the actual density. A previous observation[6] at lower energy found evidence for
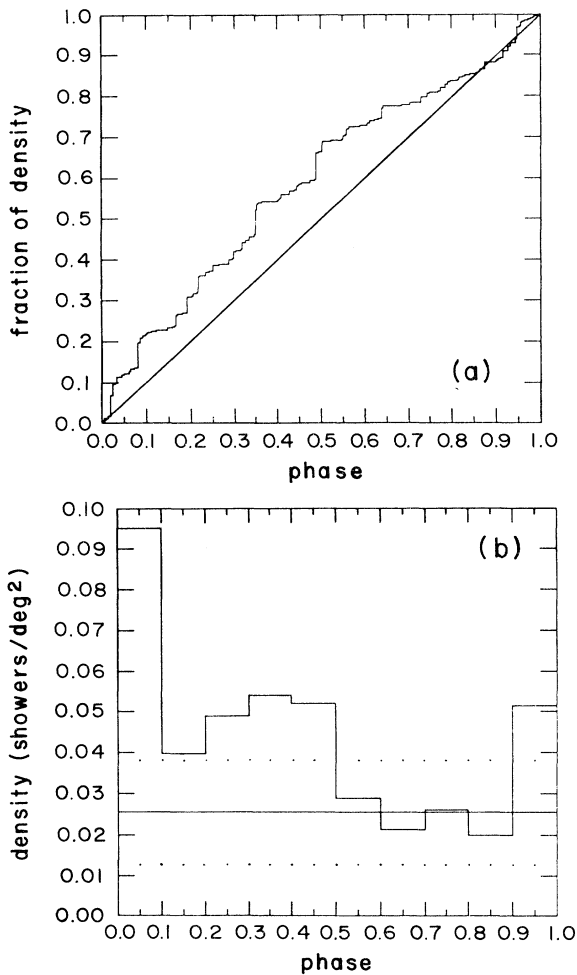
FIG. 3. (a) The full available information about the Cygnus X-3 4.8-h phase dependence by our plotting for each phase the fraction of the total density which arrived with lower phase values. The 45° line is the expected curve in the absence of periodicity. (b) The density which arrived in each of ten phase bins. The solid horizontal line shows the expected density (based on isotropic simulations), and the dotted lines indicate the rms deviation in the expected density for a single bin.
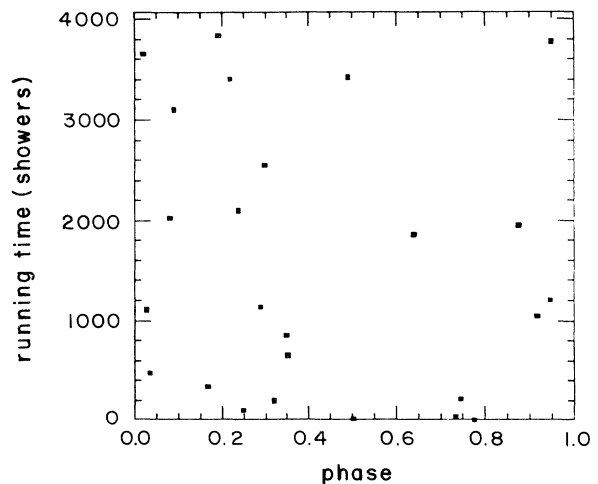

FIG. 4. Plotted are the 25 showers of highest weight contributing to the density at Cygnus X-3. The abscissa is the 4.8-h phase. The ordinate is "running time" from 0 to 4075 showers, as explained in the text.

emission near phase 0, similar to that indicated in Fig. 3. A modified Rayleigh test has been used to test for periodicity in the actual data, the modification being necessary because each shower has a weight. The Rayleigh vector is computed in the usual way, but with weighted showers. The significance is measured by performance of simulations, with the actual set of shower weights with random phases. (The cumulative Fly's Eye exposure is almost uniform in phase.[8]) The computed Rayleigh vector has a phase of 0.17 and its length is exceeded in 12% of the simulations. Figure 4 shows the 25 showers of greatest weight at Cygnus X-3. The abscissa of the plot is the 4.8-h Molnar phase. The ordinate is the Cygnus X-3 exposure time. It increases by one unit each time a shower of any energy is detected "while Cygnus X-3 is detectable." Cygnus X-3 is regarded as detectable at a shower's arrival time if it is within 45° of the zenith at that time or if its zenith angle is less than that of the shower detected. The figure suggests that Cygnus X-3 was relatively active near the start of the Fly's Eye data. The figure does not show an obvious evolution of emission phase.

Since the longitudinal development curve expected of a γ-ray shower is similar to that of a neutron-initiated shower at EeV energies, it has not been possible to determine whether the Cygnus X-3 excess is due to γ rays, neutrons, or both. A neutron flux is possible because relativistic time dilation causes the lifetime for EeV neutrons to be comparable to the speed-of-light travel time from Cygnus X-3. The probability for survival against decay is given explicitly by

$$P = \exp(-0.108D/E) \, ,$$

where D is the source distance in kpc and E is the neutron energy in EeV. If $D = 11$ kpc for Cygnus X-3, then the survival probability is 0.3 at $E = 1$ EeV, for example. Possible reasons to expect a neutron flux can be cited.[11,12]

In conclusion, there is evidence in the Fly's Eye data of neutral particles above 0.5 EeV from the direction of Cygnus X-3. This is the first direct sign of EeV cosmic-ray acceleration within the Galaxy. Additional studies at these energies may be able to resolve questions concerning the Cygnus X-3 periodicity, the type of neutral particles (neutrons or photons), spectral properties, and evolution of the flux.

[1]R. M. Baltrusaitis et al., Nucl. Instrum. Methods Phys. Res., Sect. A 240, 410 (1985).

[2]M. Samorski and W. Stamm, Astrophys. J. Lett. 268, L17 (1983).

[3]J. Lloyd-Evans et al., Nature (London) 305, 784 (1983).

[4]Review articles include T. C. Weekes, Phys. Rep. 160, 1 (1988); and R. J. Protheroe, rapporteur paper for Proceedings of the Twentieth International Cosmic Ray Conference, Moscow, 1987, edited by V. A. Kozyarivsky et al. (Nauka, Moscow, 1987).

[5]B. L. Dingus et al., Phys. Rev. Lett. 60, 1785 (1988).

[6]R. M. Baltrusaitis et al., Astrophys. J. 323, 685 (1987).

[7]V. P. Fomin et al., in Proceedings of the Seventeenth International Cosmic Ray Conference, Paris, 1981 (Centre d'Etudes Nucleaires de Saclay, Gif-sur-Yvette, France, 1981), Vol. 1, p. 28.

[8]Further details are to be published.

[9]R. M. Baltrusaitis et al., Phys. Rev. Lett. 54, 1875 (1985).

[10]Communicated via S. Corbato, L. Molnar's ephemeris (1988) is given by $T_0 = JD\ 2\,443\,052.9750 \pm 0.0006$, $P_0 = 0.199\,685\,13 \pm (1.1 \times 10^{-7})$ d, $dP/dt = (9.6 \pm 0.7) \times 10^{-10}$.

[11]L. W. Jones, University of Michigan Report No. UM-HE-88-20, 1988 (unpublished).

[12]D. Kazanas and D. C. Ellison, Nature (London) 319, 380 (1986).